

Rapid Decontamination of Chemical Warfare Agent Simulant with Thermally Activated Porous Polymer Foams

Robert B. Balow,[†] Spencer L. Giles,[‡] Christopher L. McGann,[§] Grant C. Daniels,[‡] Jeffrey G. Lundin,[‡] Pehr E. Pehrsson,[‡] and James H. Wynne^{*,‡}

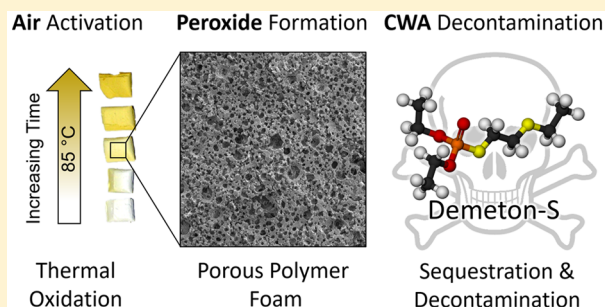
[†]National Research Council Research Associateship Program, U.S. Naval Research Laboratory, 4555 Overlook Avenue SW, Washington, DC 20375-5337, United States

[‡]Chemistry Division, U.S. Naval Research Laboratory, 4555 Overlook Avenue SW, Washington, DC 20375-5337, United States

[§]American Society for Engineering Education Postdoctoral Fellow, U.S. Naval Research Laboratory, 4555 Overlook Avenue SW, Washington, DC 20375-5337, United States

Supporting Information

ABSTRACT: Highly porous poly(dicyclopentadiene) (pDCPD) foam was synthesized via ring opening metathesis polymerization and high internal phase emulsion (HIPE) templating. Alkane and alkene moieties within the pDCPD foam oxidized slowly in air to form carbonyl, peroxy, and hydroxyl groups. Heating pDCPD to 85 °C in air accelerated the oxidation of pDCPD, producing reactive peroxy species at reduced time scales, compared to oxidation at room temperature. The oxidized pDCPD foams rapidly sequestered and decontaminated the toxic chemical warfare agent simulant, demeton-S via oxidation to vinyl, sulfoxide, and sulfone oxidation products. In addition, the porosity and high surface area of the pDCPD HIPE foams likely assists in the sequestration of demeton-S via capillary interaction. Collectively, these data demonstrate a new and highly tunable class of polymer materials capable of simultaneous sequestration and decontamination of toxic chemicals.



INTRODUCTION

Eliminating hazards associated with toxic industrial chemicals (TICs) and chemical warfare agents (CWAs) is necessary to ensure the safety of remediation personnel, and for protecting the warfighter and civilian population from such threats. Thus, the need for materials capable of automatically decontaminating toxic chemicals has spurred significant research into developing new reactive and sorbent materials and platforms.^{1–6}

An ideal decontamination material is industrially scalable, comprises inexpensive precursors, and provides rapid sequestration and decomposition of toxic compounds. Currently, metal oxides and hydroxides,^{7,8} polyoxometalates,⁹ and metal–organic frameworks^{10,11} are among the leading materials being investigated for toxic chemical remediation and CWA decontamination. Unfortunately, many of these promising compounds are cost prohibitive, because of limited industrial scalability or demonstrate reduced decontamination performance over time from interaction with atmospheric components and contaminants.^{12–14}

Polymeric materials offer a low-cost, robust, and readily tunable platform that can be exploited in numerous form factors (coatings,¹⁵ fibers,¹⁶ etc.) for toxic chemical decomposition. Polymers with hydrolytic and nucleophilic functionality, such as poly(vinyl alcohol-*co*-vinylamine), poly-

(ethylenimine), and polyacrylamidoxime, have shown effective decomposition or detoxification of many toxic chemicals and different classes of CWAs, such as blister (sulfur mustard) and nerve agents isopropyl methylphosphonofluoridate (sarin), *O*-ethyl *S*-(2-diisopropylaminoethyl) methylphosphonothioate (VX), etc.).¹⁷ Integration of such polymers into fibrous materials for self-decontaminating fabrics and wipes has also been suggested; however, the active imines, amines, and oximes suffer reduced activity when exposed to air, and must be stored under inert conditions.^{18,19}

Another common polymer, poly(dicyclopentadiene) (pDCPD), oxidizes in air to produce peroxy, hydroxyl, and carbonyl moieties.^{20,21} In this Research Note, we demonstrate that such self-generated oxidation products rapidly form at elevated temperatures in air, and quickly sequester and decontaminate the toxic CWA simulant demeton-S (*O,O*-diethyl *S*-2-(ethylsulfanyl)ethyl phosphorothioate), which is a proxy compound for the potent CWA VX (*S*-2-(diisopropylamino)ethyl *O*-ethyl methylphosphonothioate). The pDCPD oxidizes demeton-S similarly to commercial

Received: April 9, 2018

Revised: June 8, 2018

Accepted: June 14, 2018

Published: June 14, 2018

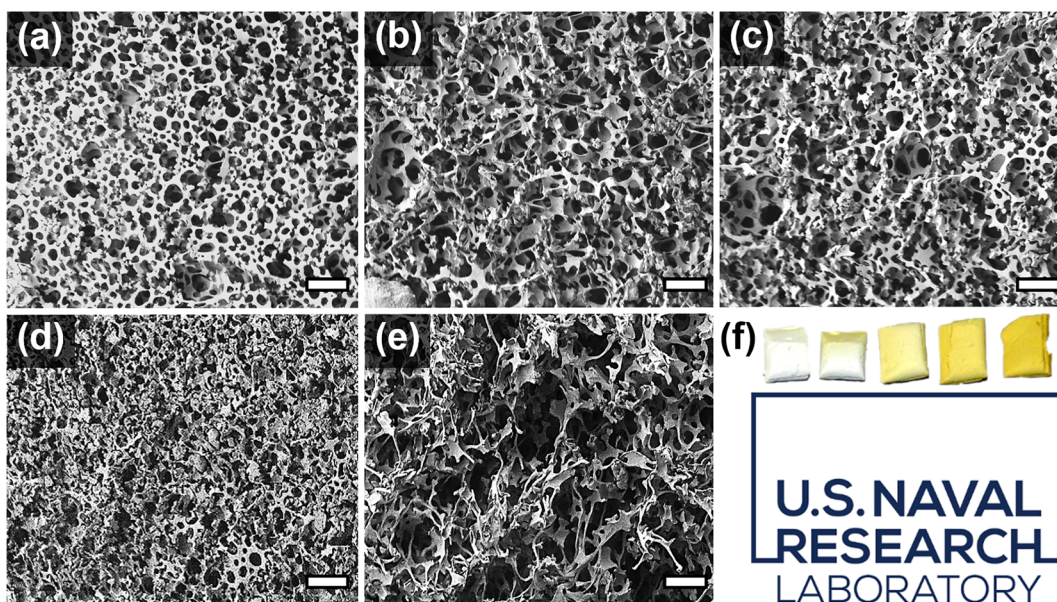


Figure 1. SEM micrographs of pDCPD HIPE foams (a) and after oxidation in air at 85 °C for (b) 1 h, (c) 2 h, (d) 4 h, and (e) 8 h. Scale bars are 10 μm . Panel (f) shows a photograph of the pDCPD foams with increasing oxidation time starting from unoxidized (left) to 8 h (right).

peroxide decontamination solutions; however, the oxidants in pDCPD remain localized to the polymer matrix. Compared to liquid peroxide-based decontamination solutions, such as Decon Green,²² which comprises 35% hydrogen peroxide,²³ the pDCPD foams greatly reduce unintended corrosion that plagues these liquid decontamination methods. In addition, polymer-bound peroxy species alleviate explosion concerns during shipping and transportation of peroxide-containing solutions. Furthermore, the morphology of pDCPD was modified using high internal phase emulsion (HIPE) templating to form porous, high-surface-area polymer networks that may assist in rapidly wicking liquid demeton-S.²⁴ This presents a new class of responsive materials capable of sequestering and decontaminating toxic chemicals within the polymer matrix that remain relatively stable for months in air under ambient conditions.²⁵

RESULTS AND DISCUSSION

The pDCPD foams were synthesized by ring-opening metathesis polymerization (see the [Supporting Information](#)),

Table 1. Change in Enthalpy Measured by DSC of pDCPD Foams Oxidized at 85 °C in Air for Various Times

oxidation time (h)	normalized heat flow (W/g)	% mass gain
0	6.3	
2	141.0	12.69
4	585.5	32.92
8	440.4	37.67

templated via HIPE, and stored under vacuum (unoxidized) or oxidized in air at 85 °C for up to 8 h. Unoxidized and oxidized pDCPD foams both show significant porosity and average pore diameters of 1–4 μm , independent of oxidation time (Figures 1a–e). The unoxidized pDCPD foams were white in color and flexible. Oxidizing in air yellowed the foams (noticeable within \sim 1 h of oxidation, Figure 1f) and increased brittleness. Large void spaces were observed for the 8 h oxidized pDCPD foams (Figure 1e); however, these voids are likely due to damage

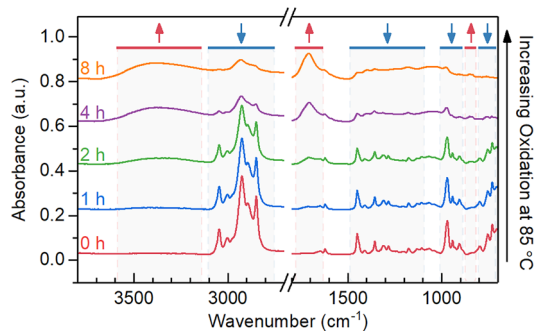


Figure 2. FTIR-ATR spectra of pDCPD foams oxidized in air at 85 °C, showing increased oxidation products (red arrows, up) and decreased alkene moieties (blue arrows, down) at longer duration.

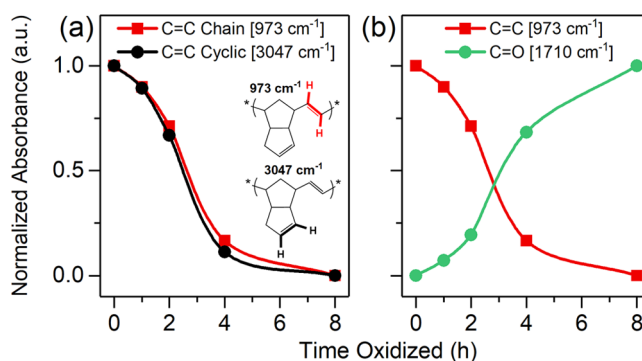


Figure 3. Normalized integrated FTIR-ATR spectra peak areas for (a) chain and cyclic alkenes and (b) chain alkenes and carbonyl oxidation products as a function of pDCPD oxidation duration. Lines are added to guide the eye.

during sample preparation resulting from the increased fragility of the oxidized pDCPD foams. The change of ductility with increasing oxidation has been previously reported.^{26,27}

The pDCPD foams heated in air at 85 °C gained almost 38% mass after 8 h (Table 1). Oxidation products indicative of carbonyl, peroxy, and hydroxyl moieties were detected by

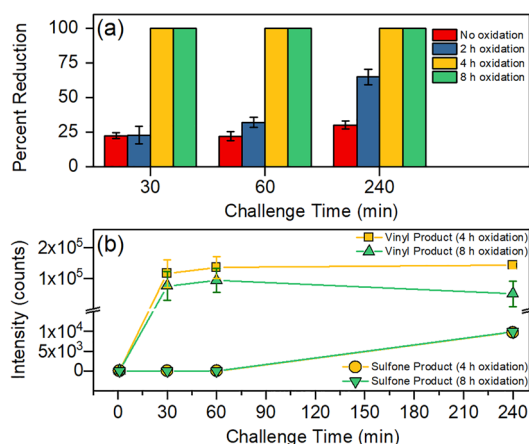


Figure 4. (a) Percent reduction of 20 μL of demeton-S/acetone solution dosed onto unoxidized and oxidized pDCPD foams, and challenged for 30, 60, and 240 min in a sealed vial. (b) GC-MS peak area of single (sulfoxide) and double (sulfone) demeton-S oxidation products with time on 4 h (yellow) and 8 h (green) oxidized pDCPD foams.

Fourier transform infrared–attenuated total reflectance (FTIR-ATR) spectroscopy (Figure 2). Saturated and unsaturated alkyl vibrational modes native to unoxidized pDCPD decreased in the collected FTIR-ATR spectra between 3100 and 2700, 1500–1100, 1000–900, and below 800 cm^{-1} with increased oxidation time (Figure 2, blue arrows). Simultaneously, bound oxidation products such as hydroxyl (3400 cm^{-1}), carbonyl (1710 cm^{-1}), and peroxy (851 and 838 cm^{-1} ; see the Supporting Information) moieties (denoted by red arrows in Figure 2) increased, which has also been reported in the literature for both elevated-temperature and room-temperature pDCPD oxidation.^{20,21,26} The lack of C–H stretching modes in the FTIR-ATR spectra near 2900 and 2800 cm^{-1} suggested the vibrational band at 1710 cm^{-1} is likely not an aldehyde moiety but a ketone. In addition, the lack of the secondary broad characteristic carboxylic acid feature near 2600 cm^{-1} further supports the ketone assignment. Chain (973 cm^{-1}) and cyclic (3047 cm^{-1}) alkene vibrational mode peak areas were integrated and plotted as a function of time (Figure 3a). Both vibrational modes decrease consistently with increased oxidation time, suggesting that alkene oxidation is nonspecific and proceeds at similar rates, regardless of whether it is derived from the alkyl backbone chain or ring. A plot of the normalized ketone versus alkene vibrational mode peak areas shows an inverse correlation with time, further supporting oxidation of the alkene moieties to ketones (Figure 3b).

Differential scanning calorimetry (DSC) analysis was performed to measure the total peroxy content within the

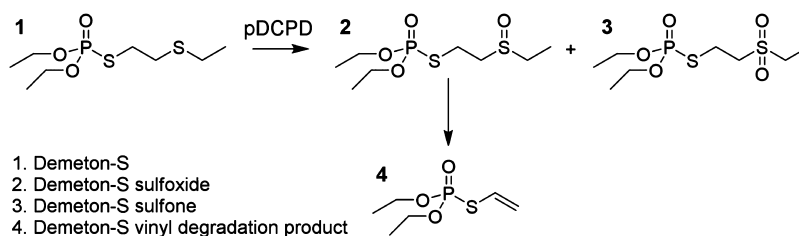
unoxidized and oxidized pDCPD foams by integrating the exotherm produced from decomposing peroxy moieties near 140 $^{\circ}\text{C}$ (see the Supporting Information).^{20,28} The calculated change in enthalpy, as well as the mass gain with time, are listed in Table 1. Unoxidized pDCPD foams contained an insignificant amount of peroxy species due to incidental air exposure (6.3 J/g). Oxidizing pDCPD at 85 $^{\circ}\text{C}$ in air for 2 h resulted in a 22-fold increase in peroxy content. The pDCPD foams oxidized for 4 and 8 h formed the most peroxy species (585.5 and 440.4 J/g, respectively). A decrease in the change of enthalpy (145 J/g) for the 8 h oxidation, compared to the 4 h oxidation indicates a reduction in total peroxy content when oxidizing beyond 4 h. The mass of the pDCPD foams continuously increased over the 8 h oxidation, suggesting that the pDCPD foams continue to form nonperoxy oxidation products beyond 4 h. Collectively, these data show the peroxide species decompose, albeit slowly, at elevated temperatures once formed. Similar peroxy losses over time have been reported in the literature.²⁸

Storage of the unoxidized foams in N_2 or vacuum at room temperature prevents the formation of oxidation products, thus providing a means for long-term storage and subsequent “activation” of pDCPD. The peroxy content of oxidized pDCPD can also be extended by storing in vacuo or under an inert atmosphere, which minimizes decomposition of the reactive peroxy species (see the Supporting Information).

Generally, more-oxidized pDCPD foam demonstrated greater decontamination of demeton-S (Figure 4a). The pDCPD foams oxidized for 4 and 8 h showed 100% reduction of demeton-S after only 30 min, whereas the unoxidized and 2 h oxidized foams exhibited $\sim 25\%$ reduction of demeton-S for 30 and 60 min challenges, attributed to trapped or sequestered demeton-S within the pores of the foams. The pDCPD foam oxidized for 2 h improved the decontamination of demeton-S by 200%, compared to the unoxidized foams challenged for 4 h. The unoxidized and 2 h oxidized pDCPD samples showed no detectable demeton-S decomposition (oxidation products) via gas chromatography–mass spectroscopy (GC-MS); however, the 4 h and 8 h oxidized pDCPD foams formed single oxidation (vinyl elimination) demeton-S decomposition products after 30 min (Figure 4b). In addition, double oxidation of demeton-S to the sulfone decomposition product was detected after a 4 h challenge. These data are promising, because demeton-S is functionally similar to the extremely lethal nerve agent VX. The use of peroxides to decompose VX is preferred, as this route avoids the formation of the very toxic hydrolysis product EA-2192.²⁹ Scheme 1 shows a proposed demeton-S oxidation mechanism.

In summary, pDCPD HIPE foams oxidized rapidly in air at 85 $^{\circ}\text{C}$ to form hydroxyl, carbonyl, and peroxy moieties that were detected using FTIR-ATR spectroscopy and DSC. Peroxy

Scheme 1. Oxidation of Demeton-S (1) by pDCPD Resulting in Oxidation Products (2 and 3) and Subsequent Elimination Product (4)



species increased with oxidation time to a maximum concentration after 4 h. A decrease of peroxy species after 8 h of oxidation indicated partial peroxy decomposition with extended pDCPD thermal oxidation. Storage of pDCPD foams in vacuum or inert atmosphere reduced the decomposition of bound peroxy species. Increased peroxy concentration within the pDCPD foams correlated with the oxidation of the toxic CWA simulant demeton-S to vinyl, sulfoxide, and sulfone decomposition products, as determined by GC-MS. In addition, the porosity of pDCPD HIPE foams likely assists in the sequestration of demeton-S, because of capillary interaction between the pores and liquid. As such, the pDCPD foams demonstrate an exciting, scalable, and low-cost material platform for rapid toxic chemical sequestration, remediation, and personnel protection applications.

■ ASSOCIATED CONTENT

📄 Supporting Information

The Supporting Information is available free of charge on the ACS Publications website at DOI: [10.1021/acs.iecr.8b01546](https://doi.org/10.1021/acs.iecr.8b01546).

Experimental procedures and details, GC-MS chromatograms, mass spectra fragmentation patterns, FTIR spectra correlations, and DSC thermograms for peroxy content and stability (PDF)

■ AUTHOR INFORMATION

Corresponding Author

*E-mail: james.wynne@nrl.navy.mil.

ORCID

Robert B. Balow: [0000-0002-2407-0105](https://orcid.org/0000-0002-2407-0105)

Jeffrey G. Lundin: [0000-0001-8605-287X](https://orcid.org/0000-0001-8605-287X)

James H. Wynne: [0000-0001-7244-9673](https://orcid.org/0000-0001-7244-9673)

Notes

The authors declare no competing financial interest.

■ ACKNOWLEDGMENTS

The authors thank the Office of Naval Research (ONR), the Defense Threat Reduction Agency (DTRA), and the U.S. Naval Research Laboratory for financial support. This research was performed while R.B.B. held a National Research Council Research Associateship award at U.S. Naval Research Laboratory. C.L.M. acknowledges funding from the American Society for Engineering Education.

■ REFERENCES

- (1) Bromberg, L.; Pomerantz, N.; Schreuder-Gibson, H.; Hatton, T. A. Degradation of Chemical Threats by Brominated Polymer Networks. *Ind. Eng. Chem. Res.* **2014**, *53*, 18761–18774.
- (2) Long, J. W.; Wallace, J. M.; Peterson, G. W.; Huynh, K. Manganese Oxide Nanoarchitectures as Broad-Spectrum Sorbents for Toxic Gases. *ACS Appl. Mater. Interfaces* **2016**, *8*, 1184–1193.
- (3) Martin, M. E.; Narske, R. M.; Klabunde, K. J. Mesoporous metal oxides formed by aggregation of nanocrystals. Behavior of aluminum oxide and mixtures with magnesium oxide in destructive adsorption of the chemical warfare surrogate 2-chloroethylethyl sulfide. *Microporous Mesoporous Mater.* **2005**, *83*, 47–50.
- (4) Peterson, G. W.; Farha, O. K.; Schindler, B.; Jones, P.; Mahle, J.; Hupp, J. T. Evaluation of a robust, diimide-based, porous organic polymer (POP) as a high-capacity sorbent for representative chemical threats. *J. Porous Mater.* **2012**, *19*, 261–266.
- (5) Singh, V. V.; Jurado-Sánchez, B.; Sattayasamitsathit, S.; Orozco, J.; Li, J.; Galarnyk, M.; Fedorak, Y.; Wang, J. Multifunctional Silver-Exchanged Zeolite Micromotors for Catalytic Detoxification of

Chemical and Biological Threats. *Adv. Funct. Mater.* **2015**, *25*, 2147–2155.

(6) Wagner, G. W.; Bartram, P. W. Reactions of VX, HD, and Their Simulants with NaY and AgY Zeolites. Desulfurization of VX on AgY. *Langmuir* **1999**, *15*, 8113–8118.

(7) Bandoz, T. J.; Laskoski, M.; Mahle, J.; Mogilevsky, G.; Peterson, G. W.; Rossin, J. A.; Wagner, G. W. Reactions of VX, GD, and HD with Zr(OH)₄: Near Instantaneous Decontamination of VX. *J. Phys. Chem. C* **2012**, *116*, 11606–11614.

(8) Balow, R. B.; Lundin, J. G.; Daniels, G. C.; Gordon, W. O.; McEntee, M.; Peterson, G. W.; Wynne, J. H.; Pehrsson, P. E. Environmental Effects on Zirconium Hydroxide Nanoparticles and Chemical Warfare Agent Decomposition: Implications of Atmospheric Water and Carbon Dioxide. *ACS Appl. Mater. Interfaces* **2017**, *9*, 39747–39757.

(9) Giles, S. L.; Lundin, J. G.; Balow, R. B.; Pehrsson, P. E.; Wynne, J. H. Comparative Roles of Zr⁴⁺ and Ni²⁺ Wells-Dawson Hetero-metal Substituted Polyoxometalates on Oxidation of Chemical Contaminants. *Appl. Catal., A* **2017**, *542*, 306–310.

(10) Mondloch, J. E.; Katz, M. J.; Isley, W. C., III; Ghosh, P.; Liao, P.; Bury, W.; Wagner, G. W.; Hall, M. G.; DeCoste, J. B.; Peterson, G. W.; Snurr, R. Q.; Cramer, C. J.; Hupp, J. T.; Farha, O. K. Destruction of Chemical Warfare Agents Using Metal-Organic Frameworks. *Nat. Mater.* **2015**, *14*, 512–516.

(11) Wang, G.; Sharp, C.; Plonka, A. M.; Wang, Q.; Frenkel, A. I.; Guo, W.; Hill, C.; Smith, C.; Kollar, J.; Troya, D.; Morris, J. R. Mechanism and Kinetics for Reaction of the Chemical Warfare Agent Simulant, DMMP(g), with Zirconium(IV) MOFs: An Ultrahigh-Vacuum and DFT Study. *J. Phys. Chem. C* **2017**, *121*, 11261–11272.

(12) Bermudez, V. M. Effect of Humidity on the Interaction of Dimethyl Methylphosphonate (DMMP) Vapor With SiO₂ and Al₂O₃ Surfaces, Studied Using Infrared Attenuated Total Reflection Spectroscopy. *Langmuir* **2010**, *26*, 18144–54.

(13) Galhotra, P.; Navea, J. G.; Larsen, S. C.; Grassian, V. H. Carbon Dioxide (C₁₆O₂ and C₁₈O₂) Adsorption in Zeolite Y Materials: Effect of Cation, Adsorbed Water and Particle Size. *Energy Environ. Sci.* **2009**, *2*, 401.

(14) Singh, J.; Mukherjee, A.; Sengupta, S. K.; Im, J.; Peterson, G. W.; Whitten, J. E. Sulfur Dioxide and Nitrogen Dioxide Adsorption on Zinc Oxide and Zirconium Hydroxide Nanoparticles and the Effect on Photoluminescence. *Appl. Surf. Sci.* **2012**, *258*, 5778–5785.

(15) Lundin, J. G.; Giles, S. L.; Cozzens, R. F.; Wynne, J. H. Self-Cleaning Photocatalytic Polyurethane Coatings Containing Modified C60 Fullerene Additives. *Coatings* **2014**, *4*, 614–629.

(16) Gephart, R. T.; Coneski, P. N.; Wynne, J. H. Decontamination of Chemical-Warfare Agent Simulants by Polymer Surfaces Doped with the Singlet Oxygen Generator Zinc Octaphenoxypthalocyanine. *ACS Appl. Mater. Interfaces* **2013**, *5*, 10191–10200.

(17) Bromberg, L.; Creasy, W. R.; McGarvey, D. J.; Wilusz, E.; Hatton, T. A. Nucleophilic Polymers and Gels in Hydrolytic Degradation of Chemical Warfare Agents. *ACS Appl. Mater. Interfaces* **2015**, *7*, 22001–11.

(18) Chen, L.; Bromberg, L.; Schreuder-Gibson, H.; Walker, J.; Alan Hatton, T.; Rutledge, G. C. Chemical protection fabrics via surface oxidation of electrospun polyacrylonitrile fiber mats. *J. Mater. Chem.* **2009**, *19*, 2432–2438.

(19) Garg, K.; Bowlin, G. L. Electrospinning jets and nanofibrous structures. *Biomicrofluidics* **2011**, *5*, 013403.

(20) Richaud, E.; Le Gac, P. Y.; Verdu, J. Thermooxidative aging of polydicyclopentadiene in glassy state. *Polym. Degrad. Stab.* **2014**, *102*, 95–104.

(21) Lyapkov, A. A.; Gvozdkov, E. L.; Tarakanovskaya, A. N.; Tarnovskaya, O. D.; Yakovleva, Y. S. Oxidation and Structuring of Polydicyclopentadiene Thin Layers. *Procedia Chem.* **2014**, *10*, 223–228.

(22) Wagner, G. W.; Yang, Y.-C. Rapid Nucleophilic/Oxidative Decontamination of Chemical Warfare Agents. *Ind. Eng. Chem. Res.* **2002**, *41*, 1925–1928.

(23) Wagner, G. W.; Procell, L. R.; Sorrick, D. C.; Lawson, G. E.; Wells, C. M.; Reynolds, C. M.; Ringelberg, D. B.; Foley, K. L.; Lumetta, G. J.; Blanchard, D. L. All-Weather Hydrogen Peroxide-Based Decontamination of CBRN Contaminants. *Ind. Eng. Chem. Res.* **2010**, *49*, 3099–3105.

(24) McGann, C. L.; Streifel, B. C.; Lundin, J. G.; Wynne, J. H. Multifunctional polyHIPE wound dressings for the treatment of severe limb trauma. *Polymer* **2017**, *126*, 408–418.

(25) McGann, C. L.; Daniels, G. C.; Giles, S. L.; Balow, R. B.; Miranda-Zayas, J. L.; Lundin, J. G.; Wynne, J. H. Air Activated Self-Decontaminating Polydicyclopentadiene PolyHIPE Foams for Rapid Decontamination of Chemical Warfare Agents. *Macromol. Rapid Commun.* **2018**, 1800194.

(26) Kovačič, S.; Krajnc, P.; Slugovc, C. Inherently reactive polyHIPE material from dicyclopentadiene. *Chem. Commun.* **2010**, *46*, 7504–6.

(27) Le Gac, P. Y.; Choqueuse, D.; Paris, M.; Recher, G.; Zimmer, C.; Melot, D. Durability of polydicyclopentadiene under high temperature, high pressure and seawater (offshore oil production conditions). *Polym. Degrad. Stab.* **2013**, *98*, 809–817.

(28) Defauchy, V.; Le Gac, P. Y.; Guinault, A.; Verdu, J.; Recher, G.; Drozdak, R.; Richaud, E. Kinetic analysis of polydicyclopentadiene oxidation. *Polym. Degrad. Stab.* **2017**, *142*, 169–177.

(29) Kim, K.; Tsay, O. G.; Atwood, D. A.; Churchill, D. G. Destruction and Detection of Chemical Warfare Agents. *Chem. Rev.* **2011**, *111*, 5345–5403.